

---

# AUTOMATED HIGH-PRECISION EXTRACTION AND FORENSIC VERIFICATION OF DATA-BEARING VECTOR FIGURES

---

PREPRINT

**Bowen Sun\***  
Johns Hopkins University  
bsun39@jh.edu

**Chaowei Xiao**  
Johns Hopkins University  
chaoweixiao@jhu.edu

Code and data: [github.com/Bowen-Sun-0728/figverify](https://github.com/Bowen-Sun-0728/figverify)

## ABSTRACT

The quantitative record of science and engineering is increasingly carried by figures rather than text or tables, and a reader who needs the underlying numbers must usually re-digitize them by hand: slowly, imprecisely, and with no way to prove the result is faithful. Yet when a figure is stored as vector graphics, its data are not approximated by the picture but encoded in it: the renderer writes each marker and vertex at a printed precision that, for the dominant scientific toolchain, exceeds the data's own. We turn this into three contributions, one per shortcoming of hand digitization. First, a precision theory bounding how accurately data can be recovered for a given renderer and export format: bit-exact `Float32` for `matplotlib` markers, and a calibration-limited three to four significant figures end to end. Second, an automatic extractor that decodes a figure in one pass with no human in the loop, in place of the slow point-by-point tracing a digitizer demands. Third, a verification theory: recovery is injective except on a characterized, vanishingly small interval near zero; accidental agreement between unrelated data is astronomically unlikely; and a re-rendering certificate binds the recovered values to the markers, lines, and ticks the figure draws, not its text, making a result non-repudiable. With no ground truth used during recovery, decoded figures match external archives (Planck 2018 to  $\sim 10^{-9}$ ; the Keeling  $\text{CO}_2$  record to  $\sim 5 \times 10^{-4}$ ), and one decoded figure independently reproduces a correction to the Chinchilla scaling-law confidence interval. We map the achievable precision across common renderers and their PDF, SVG, and EPS formats. What we deliver is certified data; the scientific significance of any particular dataset lies outside this paper's scope, and recovered values are candidates for human review, never accusations.

**Keywords** vector graphics · PDF · data extraction · reproducibility · matplotlib · document forensics · floating point

## 1 Introduction

A growing share of scientific and engineering results now reaches the reader as a picture. A scaling law is a line through a cloud of points; a measured spectrum is a curve with error bars; a device characteristic is a family of curves on a datasheet. The numbers behind these pictures are often not printed in the surrounding text, nor supplied as a table, nor deposited as data: the figure itself is the record. A reader who wants those numbers, whether to reproduce an analysis, combine results across papers, or check a headline claim, is forced to recover them from the figure.

Today that recovery is done by hand, with a mouse, in tools that ask the user to click along a curve or trace a point cloud [1]. This practice has three deficiencies, and they motivate everything that follows.

**(D1) Low precision.** Hand-digitization recovers perhaps two or three significant figures, set by how steadily a human can place a cursor over a rasterized image. The recovered numbers inherit no stated error and no provenance.

---

\*Corresponding author.

**(D2) Low automation, hence low throughput.** Because a person is in the loop for every point, the cost scales with the data. Digitizing one figure is tedious; digitizing the thousands of figures needed for a meta-analysis, an audit, or a corpus study is infeasible.

**(D3) No verification.** Even a carefully digitized dataset cannot be proven to be the numbers the author actually plotted. Hand digitization offers no certificate of its own fidelity, and so no non-repudiable result that a third party is compelled to accept.

The key observation of this paper is that, for an important class of figures, none of these deficiencies is fundamental. When a figure is stored as vector graphics (the default for the  $\text{\LaTeX}$ -authored physics, astronomy, and computer-science literature, and for many engineering datasheets), the document does not contain an image of the plot. It contains the drawing instructions: the exact device coordinates of every marker, the vertices of every polyline, the geometry of every axis tick. The renderer wrote those coordinates with a fixed number of decimal places that, for the dominant scientific toolchain, resolves more finely than the data’s own numerical type [2]. The data are therefore not approximated by the figure; they are encoded in it, and can be decoded automatically, to high precision, and with a certificate.

Extracting data from vector charts is not itself new [1, 3, 4], and the observation that vector figures carry more numerical information than raster ones has been made before, including in a notable manual forensic reanalysis of a single disputed result [5]. Our contribution is not the possibility of extraction but its formalization, automation, certification, and characterization. Concretely, mirroring the three deficiencies above:

- **A precision theory (addresses D1; Section 4).** We show that the achievable accuracy is governed by two separable steps, the renderer’s coordinate quantization and the reader’s axis calibration, and we bound each. For `matplotlib`’s PDF backend the quantization step returns bit-exact `Float32`; calibration is then the true bottleneck, at three to four significant figures, which already exceeds what most papers report for the same quantities.
- **An automatic extractor (addresses D2; Section 6).** A white-box parser paired with a black-box re-render decodes a figure in a single automatic pass, with no human in the loop, in place of the slow point-by-point tracing a digitizer requires; because nothing is interactive, the cost no longer grows with the number of points, and the same step runs over many figures as easily as over one.
- **A verification theory (addresses D3; Section 5).** The core is a proof that the extraction itself is correct. Recovery is injective except on a characterized, vanishingly small interval near zero, and accidental agreement between unrelated data is astronomically unlikely, so when the recovered values re-render to the same markers, lines, and ticks the figure draws they are certified to be the data that produced the figure: a non-repudiable result. That the same certificate also exposes a figure altered after rendering is a secondary benefit.

We support the theory with results that need no trust. With no ground truth used during recovery, decoded figures agree with independent public archives (Planck 2018 to  $\sim 10^{-9}$  and the Keeling  $\text{CO}_2$  record to  $\sim 5 \times 10^{-4}$ , Section 7), and we measure the achievable precision across common renderers and their PDF, SVG, and EPS export formats (Section 8). As a concrete and deliberately safe application, we decode the figure behind the Chinchilla scaling law and independently reproduce a published correction to its confidence interval (Section 9). We release `FIGVERIFY`, an open-source verifier. Because decoding figures at this precision could power a range of data-integrity checks, from spotting fabricated or altered points to detecting reuse across figures, we are explicit about scope: this paper concerns only the extraction and its verification, and passes no judgement on the integrity of any particular figure or paper. As detailed in Section 10, recovered values are candidates for human review, never automated accusations.

## 2 Related work

We position our work against four lines of prior art. In each case the prior method is real and useful; we state what it does and then the specific advantage our approach adds, indexed to the deficiencies of Section 1.

**Interactive raster digitizers.** Tools such as `WebPlotDigitizer` [1] let a user recover approximate data by clicking on a rasterized plot. They are general (they work on any image) and widely used. But they are semi-automatic (a human places points) and pixel-limited (precision is set by image resolution and hand steadiness), and they produce no certificate. Our advantage is fully automatic recovery at the renderer’s native precision, with a re-render certificate, directly answering D1–D3, at the cost of requiring a vector source.

**Vector-chart extraction.** `ChartDetective` [3] and `svgdigitizer` [4] recover data from vector charts (PDF or SVG), and are far more accurate than raster digitizers because they read coordinates rather than pixels. They remain, however,

interactive (the user identifies series, axes, and mappings) and they treat extraction as an engineering task rather than a quantity with a provable ceiling. Our advantage is a precision theory that says how many bits are recoverable for a given renderer and format (Sections 4 and 8), automation of series and axis identification, and a certificate on the output. We also show that the common PDF→SVG conversion route used by such pipelines discards roughly ten to fourteen bits relative to parsing the PDF directly (Section 8).

**Raster image forensics.** A large literature detects manipulated bitmap figures, the duplicated or spliced blots and micrographs typified by large-scale screening for inappropriate image reuse [6]. This work is essential where the figure is a photograph, but it operates on pixels and does not recover the plotted numbers, so it cannot check whether a curve is consistent with a claim. Our advantage is that for vector plots we recover the numerical data and bound the probability that an apparent match is coincidental, giving a quantitative, data-level forensic primitive rather than a pixel-level one.

**Manual forensic reanalysis.** Most directly related, Hamlin [5] manually digitized a disputed condensed-matter figure (via a PDF→SVG centroid extraction) and used the recovered digital precision to argue about data provenance, demonstrating, by hand and on a single case, that vector figures carry forensically meaningful information. That work validates its recovered numbers only indirectly, though, by comparison with external ground truth and by concordance across a few related figures and renderings; it offers no direct verification mechanism, no certificate that an extraction is correct on its own terms. None of the prior art above does. A central original contribution of this paper is exactly such a mechanism: a re-rendering certificate that ties the recovered values to the markers, lines, and ticks the figure itself draws and so proves an extraction faithful without recourse to any outside reference. Around it we add the formal recoverability theory, the no-collision guarantee, the ground-truth validation against external archives, and the map across renderers and formats that together turn a one-off manual analysis into a general, automatic method.

In short, neither high-precision vector extraction nor the idea that vector figures are forensically informative is new. What we add is the theory that bounds the precision, the automation that scales it, the measurements that delimit where it works, and, above all, the verification certificate that makes a recovered result provable rather than merely plausible.

### 3 Preliminaries

We first describe, in renderer-agnostic terms, the pipeline that turns numbers into a vector figure, since it is this pipeline, not any one library, that determines what can be recovered. `matplotlib` appears only as a concrete instance.

**From data to device coordinates.** A plotting library places a data value on the page by an affine map. For a single axis, a data value  $v$  becomes a device coordinate

$$u = av + b, \tag{1}$$

where the scale  $a$  and offset  $b$  are fixed by the axis limits and the physical size of the plotting area; a log axis applies Equation (1) to  $\log v$ . The pair  $(a, b)$  is shared by every datum drawn against that axis, and the axis ticks are themselves drawn through the same map, a fact we will use to recover  $(a, b)$  without any external information.

**From device coordinates to stored text.** The vector container (PDF, SVG, or EPS) is a program: it records drawing operators and their operands as text. A point at device coordinate  $u$  is therefore written as a decimal numeral with a fixed number of fractional digits set by the backend. Writing  $d$  fractional digits snaps  $u$  to a grid of spacing

$$\Delta_s = 10^{-d} \tag{2}$$

in the coordinate unit; we call  $\Delta_s$  the storage quantum. Crucially, the data value is not rounded to “plot resolution”; it is rounded only at this final printing step, which is typically far finer than the eye, and (as we will see) often finer than the data’s own numerical type.

**Markers, polylines, and series.** Two drawing primitives carry essentially all plotted data. A marker (a scatter point) is a small glyph placed at a point; a polyline (a line plot) is a connected sequence of vertices. Backends commonly emit the points of one series as an absolute first placement followed by incremental offsets, so recovering positions requires accumulating those increments per series, a detail that matters for correctness (Section 6) but not for the precision argument.

**The matplotlib instance.** In `matplotlib`’s PDF backend, marker centres are placed through a coordinate-system transform written with ten fractional digits ( $d = 10$ ,  $\Delta_s = 10^{-10}$ ), while polyline vertices are written with six ( $d = 6$ ,  $\Delta_s = 10^{-6}$ ). These two numbers, together with the affine map of Equation (1), are all the precision theory of Section 4 needs. Other renderers and export formats choose different  $d$ , and we tabulate the consequences in Section 8.

**What “recovery” means.** Given the stored coordinates and an estimate  $(\hat{a}, \hat{b})$  of the affine map, we invert Equation (1) to obtain  $\hat{v} = (\tilde{u} - \hat{b})/\hat{a}$ . The rest of the paper asks two questions about  $\hat{v}$ : how close it is to  $v$  (Section 4), and when a match between recovered values can be trusted as non-coincidental (Section 5).

## 4 Extraction precision

We now bound the accuracy of the recovered value  $\hat{v}$ . Two quantization steps stack, and the coarser one dominates; the surprising empirical fact is which one it is.

### 4.1 The two-step ceiling

We first fix the two steps precisely. A datum  $v$  is placed at  $u = av + b$  (Equation (1)) and stored by rounding to the grid Equation (2), so the stored coordinate is  $\tilde{u} = u + \eta$  with  $|\eta| \leq \frac{1}{2}\Delta_s$ . The affine map is not known exactly but recovered from the axis ticks as  $\hat{a} = a(1 + \delta_a)$  and  $\hat{b} = b + \Delta_b$ , with the calibration error collected into a single relative quantity  $\varepsilon$  such that  $|\delta_a| \leq \varepsilon$  and  $|\Delta_b| \leq \varepsilon|b|$ . Recovery inverts the estimated map,  $\hat{v} = (\tilde{u} - \hat{b})/\hat{a}$ .

**Theorem 1** (Extraction-precision ceiling). *With the setup above, the recovered value obeys*

$$|\hat{v} - v| \leq \underbrace{\frac{\Delta_s}{2|a|}}_{\text{storage step}} + \underbrace{\varepsilon(|v| + |b/a|)}_{\text{calibration step}} + O(\varepsilon^2), \quad (3)$$

where the storage step is fixed by the renderer and format, and the calibration step by what the reader can reconstruct of the axes.

We prove this in Section A. The content of Theorem 1 is that the achievable error is the sum of the two terms, dominated by whichever is larger, and that the two have very different sizes in practice.

### 4.2 A worked matplotlib example

Consider a scatter plot drawn by `matplotlib`’s PDF backend on a panel a few inches wide. The marker storage quantum is  $\Delta_s = 10^{-10}$  in the transformed unit, and the scale  $a$  maps the axis range onto that panel. Plugging real values into the storage term of Equation (3), the half-ulp of storage lands below the spacing of the `Float32` grid over the entire plotted range: inverting the stored coordinate returns the very same `Float32` number the library started from, bit for bit, all 24 bits of significand [7], not an approximation of them. We confirm this directly in Section 7: against data we control, marker recovery is exact to the last bit; against Planck’s released spectrum it agrees to  $\sim 10^{-9}$ , i.e. to the `Float32` floor.

Polylines are coarser. With  $\Delta_s = 10^{-6}$  the storage term caps a polyline vertex at roughly six to seven significant figures, still far beyond what any hand digitizer reaches, but no longer bit-exact.

### 4.3 Calibration is the real bottleneck

The second term of Equation (3) is the one that bites. In practice the reader does not know  $(a, b)$  exactly; they are recovered from the tick marks, whose device positions are themselves only stored coordinates, and whose data values are read from the tick labels, whose printed precision sets the true limit (Section C). This injects a relative error  $\varepsilon$  of order  $10^{-3}$  to  $10^{-4}$  of the axis range. Since  $\varepsilon \gg \Delta_s/|a|$  for any real figure, the calibration term dominates and

$$|\hat{v} - v| \approx \varepsilon(|v| + |b/a|) \sim 10^{-3}\text{--}10^{-4} \text{ of the axis range,}$$

i.e. three to four significant figures end to end. This is the number a user of the method actually gets. Two remarks make it meaningful. First, it is not a limitation of the figure: the data are stored far more precisely, and better calibration (more ticks, a known axis transform, or author-supplied limits) moves the ceiling back toward the storage floor. Second, three to four significant figures already exceeds what most papers report for the same quantities, so even the calibration-limited result is often more precise than the text it accompanies. We return to this in Section 7, where the Keeling polyline, in the calibration-limited regime, reproduces the reference record to  $\sim 5 \times 10^{-4}$ , exactly the regime Equation (3) predicts.

The storage term, finally, is renderer-specific: it is what separates a backend that resolves the `Float32` grid from one that does not. We quantify that across the ecosystem in Section 8.

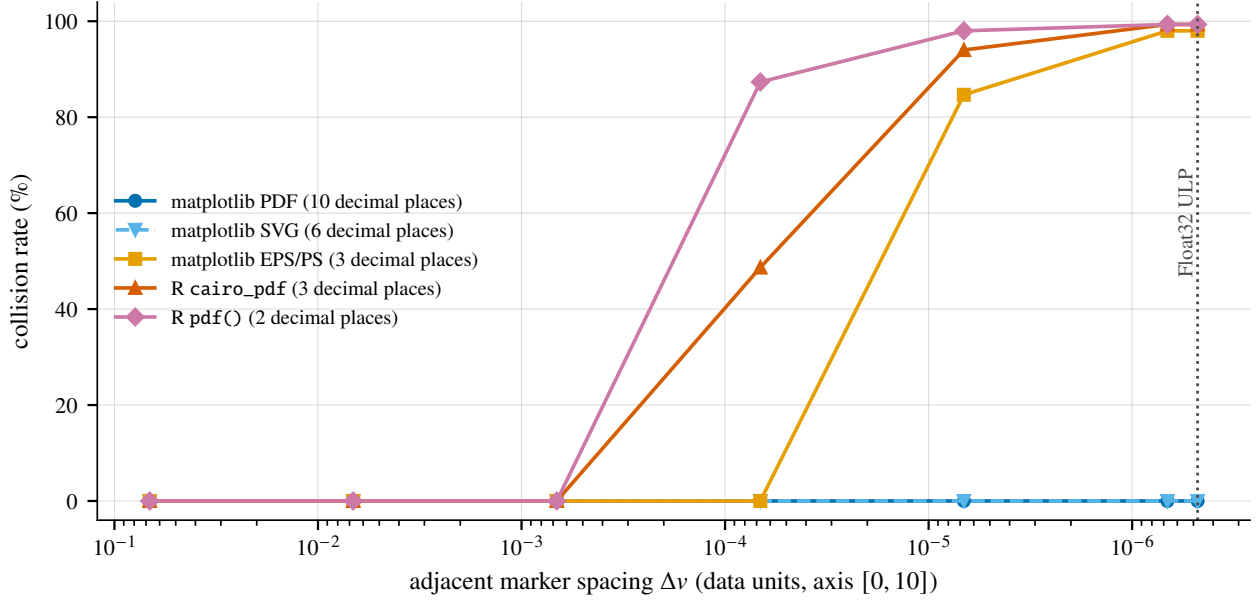


Figure 1: Injectivity, measured. We pack 150 distinct values into a shrinking window on a fixed axis, render them with each renderer, and re-extract; a collision is two distinct inputs that land on one stored device coordinate (Theorem 2). As the adjacent spacing  $\Delta v$  falls below a renderer’s storage quantum, collisions appear. matplotlib’s PDF and SVG outputs (ten and six decimal places) resolve every marker down to the Float32 ULP with no collisions, and coincide along the bottom axis, whereas matplotlib’s EPS/PS output (three decimals) and both R devices collapse, keeping only a handful of distinct values out of 150 at tight spacing. The same library loses most of its precision through the PostScript backend, so format matters as much as renderer. This is the renderer contrast of Section 8 at the level of individual points.

## 5 The no-collision property

This section is what lets the method’s forensic conclusions be stated rigorously rather than suggestively. Recovering a number accurately is not enough to use it as evidence; two further things must hold. First, the recovery must be unambiguous: two different data values must never end up stored as the same coordinate, or we could not say which one the author plotted. Second, an agreement must be meaningful: if a recovered dataset coincides with another figure or a published reference, that coincidence has to be far too unlikely to be chance. We call the first property injectivity and the second a coincidence bound, and together they are what we mean by “no collision”. Without them a forensic match is only a plausible story; with them it becomes evidence. The two subsections make each precise.

### 5.1 Injective recovery, and the interval where it fails

**Theorem 2** (Injectivity and the collision interval). *Two distinct data values are stored as distinct coordinates whenever their device separation exceeds the storage quantum,  $|a| |v_1 - v_2| > \Delta_s$ , and may collide only when it does not. Consequently recovery is injective on any data whose neighbouring values are separated by more than  $\Delta_s/|a|$ . If the data are Float32 numbers, the representable grid at magnitude  $|v|$  has spacing  $\text{ulp}(v) = 2^{\lceil \log_2 |v| \rceil - 23}$ , so individual values are resolvable when  $|v| > x^\dagger$ , where*

$$x^\dagger \approx \frac{\Delta_s}{|a|} 2^{24}. \quad (4)$$

*Below  $x^\dagger$ , a dyadic interval  $[-x^\dagger, x^\dagger]$  around zero, the floating-point grid is finer than the storage grid and neighbouring values collide.*

The proof and the exact dyadic constant are in Section B. Figure 1 demonstrates the injectivity condition directly on real renders: as markers are packed below a device’s storage quantum, distinct inputs begin to land on one stored coordinate, and the onset is set by that device’s measured quantum.

**The failure interval is rare, and rarity is renderer-specific.** The width of  $[-x^\dagger, x^\dagger]$  scales with the storage quantum, so the renderer decides how often it matters. For matplotlib PDF, Equation (4) gives  $x^\dagger \approx 4 \times 10^{-6}$  of the axis range, so a datum must sit within about 0.0004% of zero to be at risk, which essentially never happens for data plotted on a sensibly chosen axis. For PGFPlots the interval reaches `Float32` only near the top of the scale. For R’s PDF devices, by contrast,  $x^\dagger$  exceeds the entire axis range, so these devices never resolve the `Float32` grid and collisions are pervasive at that level, exactly as Figure 1 shows. The point is that for the backend on which bit-exact recovery is claimed, the collision region is a vanishing sliver, not a common occurrence.

## 5.2 A match is evidence, not coincidence

The second sense of “no collision” is statistical, and it is what gives the method forensic force. Suppose two figures, or a figure and a reference dataset, share  $n$  recovered points. If those points are genuinely unrelated, how likely is the agreement to be accidental?

**Theorem 3** (Coincidence bound). *Suppose each matched coordinate carries  $b$  effective bits: after degenerate, low-cardinality, and structured values are excluded, it is modelled, against an adversary seeking a chance match, as no more concentrated than uniform over its  $2^b$  resolvable cells. Let two point sets of size  $n$  be independent, with the two coordinates of a point independent, and call two points matched when both coordinates agree to within one cell. Then the probability that all  $n$  points of one set match the other is at most*

$$\Pr[\text{accidental match}] \leq 2^{-2nb}. \quad (5)$$

For modest values this is astronomically small:  $n = 20$  points at  $b = 10$  effective bits gives  $2^{-400} \approx 10^{-120}$ . A multi-point agreement is therefore not something that happens by chance; it is evidence that the two figures share a common data origin, or that a recovered figure faithfully reproduces the reference. We use Equation (5) in two ways: to certify a recovery (a decoded figure whose re-render reproduces the original’s markers, lines, and ticks agrees on every point, an event of negligible coincidence probability) and to flag genuine data reuse across figures.

**Why all points, not one.** The force of Equation (5) comes from requiring all  $n$  points to agree at once, not from any single coincidence. A lone match carries little weight: two unrelated series land on the same value at one point with probability about  $2^{-2b}$ , which for the  $b = 10$  above is roughly  $10^{-6}$ , small but not rare once a whole corpus is scanned. Asking instead whether some one of the  $n$  points happens to coincide is the wrong test: that probability grows with  $n$ , to about  $n 2^{-2b}$ , and is exactly the rate of accidental single matches the method must rise above. Requiring simultaneous agreement on the entire set behaves the opposite way: every further point multiplies the improbability, so  $n$  points give  $2^{-2nb}$  and the evidence compounds. A single coincidence is noise; agreement on all  $n$  points together is the signal, which is why both the certificate and the reuse test demand the whole set, never a part of it.

**The entropy gate.** Bound Equation (5) is only as strong as  $b$ . Integer-valued, low-cardinality, or otherwise structured sequences carry few effective bits, and unrelated figures can share them by chance; two plots both running  $1, 2, \dots, 10$  on the  $x$ -axis is not evidence of anything. We therefore gate the forensic test to high-entropy sequences, estimating  $b$  per series and excluding the degenerate cases before any claim is made. This gate is what keeps a large bound from becoming a false accusation, and it is applied uniformly in Section 7.

## 6 Implementation

Our verifier, FIGVERIFY, is a white-box parse paired with a black-box re-render. We describe the steps that bear on precision and on the certificate, and summarise axis calibration here while deferring its details to Section C; the lower-level page plumbing, walking the page tree and tracking the graphics state, is standard and we pass over it.

**Reading coordinates without losing bits.** The decisive choice is to parse the vector container directly, never through a conversion. We read the page content stream and follow the graphics state through nested form XObjects, collecting the operands of the marker- and line-drawing operators as written, at the backend’s full  $d$  fractional digits (Equation (2)). This is what preserves the storage floor of Section 4: as we quantify in Section 8, routing through PDF→SVG (a common shortcut) re-quantizes the coordinates and discards roughly ten to fourteen bits, collapsing bit-exact recovery into mere digitization.

**Reconstructing series.** Because backends emit a series as an absolute first point followed by incremental offsets, we segment the stream into per-series blocks and reconstruct positions by a cumulative sum within each block. Getting this segmentation right is necessary for correctness, since an off-by-one in the accumulation corrupts an entire series, but it introduces no error of its own: the arithmetic is exact in the stored precision.

**Calibrating the axes.** The affine map is recovered from the ticks the renderer itself drew, with no axis limits or metadata assumed. We segment the page into panels from the drawn frames, collect the text spans below and to the left of each panel as candidate tick labels, and parse them into values, recombining a base “10” with its raised exponent into  $10^k$ , expanding SI suffixes such as “1B” or “10T”, and reading scientific notation directly. From the resulting (position, value) pairs we fit a linear and a logarithmic map and keep the one with the smaller residual, which also serves as a quality gate: a panel that does not fit cleanly is reported as uncalibrated rather than guessed. Section C gives the full procedure and identifies tick-label rounding as the dominant source of the calibration error  $\varepsilon$  of Equation (3).

**Inverting the quantization.** With coordinates in hand and the affine map recovered, we invert Equation (1). When the backend resolves the `Float32` grid (Section 8) and calibration is tight, we additionally snap to the unique `Float32` pre-image, recovering the exact value the author held in memory; when it is not, we report the digitized value with the precision Equation (3) allows. Calibration, the practical bottleneck (Sections C and 4), contributes only the  $\varepsilon$  term already accounted for.

**Certifying by re-rendering.** Recovery alone is not a proof. We therefore re-render the recovered data with the same library and compare the result against the original at the byte level, but only over the elements that carry data: the marker placements, the polyline vertices, and the axis-tick geometry, matched operator for operator. The comparison deliberately excludes everything that encodes no plotted value, the text of axis labels, titles, and annotations, the embedded fonts, and the document metadata, since two faithful renders can differ in these without differing in the data, and folding them in would only weaken the test. Agreement on the data-bearing operators is the certificate: by the coincidence bound Equation (5) it cannot arise unless the recovered data are the plotted data, so the result is non-repudiable. The same comparison makes tampering evident: an edit to the plotted geometry after the original render cannot reproduce those operators without the original data, closing the loop between what we decoded and what the document contains. The one assumption is that the original’s renderer can be reproduced; matplotlib’s content stream is stable across releases, so in practice re-rendering matches without knowing the exact version.

**Cost.** Every step is linear in the number of drawn primitives and involves no human interaction, so the verifier runs unattended over large collections; this is the automation that answers deficiency D2 of Section 1.

## 7 Results

The strongest test of a decoder is to decode a published figure whose underlying data exist in an independent public archive, without using that archive during recovery, and then compare. We do this in the two regimes predicted by Section 4: markers, the machine-precision regime, and polylines, the calibration-limited regime. In both, the recovered data match the reference, and the few residual discrepancies are explained by the theory rather than signalling a failure of the method. Both flagship figures are matplotlib PDFs, the one backend that resolves the `Float32` grid (Section 8); on other renderers the machine-precision regime is unavailable and recovery falls to the lower, calibration-limited ceilings mapped there, so the bit-exact result below is matplotlib-specific while the polyline result is representative of any vector backend.

**Markers: the machine-precision regime.** The Planck 2018 temperature power spectrum [8] is published as both a figure and a data release. Decoding the figure’s markers and calibrating from its ticks reproduces the released multipole and power pairs to  $\sim 10^{-9}$ , the `Float32` floor anticipated in Section 4. No Planck data entered the pipeline. Against figures we generate ourselves, where the ground truth is known exactly, marker recovery is bit-exact: the recovered `Float32` values equal the inputs on every bit, consistent with Theorem 1 and with the injectivity of Theorem 2.

**Polylines: the calibration-limited regime.** The Keeling  $\text{CO}_2$  curve, as plotted in a recent preprint, decodes to the NOAA Mauna Loa monthly record [9] to  $\sim 5 \times 10^{-4}$  of range. This is not a shortfall of the figure but the calibration term of Equation (3) made visible: a smooth polyline offers fewer independent constraints on the affine map than a field of discrete markers, so the calibration error is larger. The residual is consistent with tick-calibration error and with nothing in the stored curve.

**Explaining the exceptions.** Where individual points disagree with the reference, the cause is always one of the mechanisms the theory names, never an unexplained failure: values inside the dyadic interval  $[-x^\dagger, x^\dagger]$  of Theorem 2, where neighbouring floats are genuinely unresolvable; calibration error on figures with sparse or ambiguous ticks, bounded by Equation (3); and points occluded by overplotting, which the parser flags rather than guesses. Each is predicted, each is detectable, and each shrinks under better calibration, so the agreement with ground truth is not only close but accountable. Beyond these two flagship cases, a larger audit of recovered figures against their deposited

Table 1: Precision by renderer and export format.  $B_{\text{extract}}$  is the significand bits recoverable at full scale (defined above); “Resolves Float32?” asks whether that exceeds the 24-bit Float32 grid, the condition for recovering the exact stored value; the “(provenance)” tag marks the stronger case where the headroom above 24 bits also fingerprints the render. The last column is a measured round-trip error: the median relative error between recovered and true values. Top block: a controlled round-trip (render the same known dataset, re-extract, fit the affine map, take the residual), which exposes each renderer’s storage floor and confirms the  $B_{\text{extract}}$  ceiling (the error tracks  $2^{-B_{\text{extract}}}$ ; matplotlib PDF recovers Float32 bit-for-bit). Bottom block: renderers we could not run locally, measured instead on a real published figure with deposited data, where calibration rather than storage sets the floor (Section 4) and the error is sub-percent. EPS/PS is Encapsulated PostScript; matplotlib writes only three marker decimals there, so its PostScript output falls below the Float32 grid.

Renderer	Format	$B_{\text{extract}}$	Resolves Float32?	Round-trip error
matplotlib	PDF	$\sim 42$	yes (provenance)	$3 \times 10^{-13}$ (bit-exact)
matplotlib	SVG	$\sim 32$	yes	$8 \times 10^{-10}$
matplotlib	EPS/PS	$\sim 19$	no	$9 \times 10^{-7}$
PGFPlots / TikZ	PDF	$\sim 25$	borderline	$4 \times 10^{-8}$
R cairo_pdf	PDF	$\sim 18$	no	$3 \times 10^{-6}$
R pdf()	PDF	$\sim 14.5$	no	$7 \times 10^{-6}$
Measured on a real published figure (calibration-limited; not run locally):				
MATLAB		from a deposited-data figure		0.12%
OriginLab		from a deposited-data figure		0.25%

source data, across several renderers, gives a median relative error of about 0.09%, in the calibration-limited regime; the MATLAB and OriginLab rows of Table 1 are two figures from this audit, while that table’s top block reports separate controlled round-trips that isolate each renderer’s storage floor.

## 8 Renderer and format coverage

The storage term of Equation (3) is a property of the exporter, not of the plotting library’s intent, so the right unit of analysis is the pair (renderer  $\times$  export format). Table 1 characterizes coverage on a single bit scale: for each pair it reports the storage precision and a measured round-trip error.

We read the table two ways. The extractable precision  $B_{\text{extract}} = \log_2(\text{axis span}/\Delta_s)$  is the recoverable significand at full scale, that is, how accurately data can be liberated. Forensics needs more, in two grades. Recovering the exact stored Float32 value requires only  $B_{\text{extract}} > 24$ , the significand depth, a bar SVG clears and PGFPlots reaches. Provenance fingerprinting is stronger: it requires enough headroom above 24 bits for the recovered data to re-render to the original page bytes, and only matplotlib PDF, at about 42 bits, has it.

**What the table says.** Three points stand out. First, format matters as much as renderer: the same matplotlib data recovers Float32 bit-for-bit through the PDF backend (ten marker decimals) and to nine digits through SVG (six decimals), but collapses to three or four significant figures through the PostScript backend (three decimals), below the Float32 grid. Second, only matplotlib PDF pairs full Float32 recovery with the extra headroom (about 42 bits) that fingerprints provenance; SVG and PGFPlots reach Float32-grade data recovery but not provenance. Third, the controlled round-trips track  $2^{-B_{\text{extract}}}$  and so confirm the storage ceilings, whereas real published figures round-trip only to sub-percent accuracy because there calibration, not storage, sets the floor, exactly as Section 4 predicts; the median over our ground-truth audit is about 0.09%.

**Beyond the table.** Two pipeline facts sit alongside these renderers. Converting a PDF to SVG with pdf2svg re-quantizes matplotlib’s markers to about 28 bits, which is the route behind the manual reanalysis of Hamlin [5] and why FIGVERIFY parses PDF directly (Section 6); and Plotly writes seven decimals but its Skia backend caps effective precision near Float32. Our extractor also handles ROOT, gnuplot, xmgrace, Mathematica, IgorPro, and Adobe Illustrator figures at the digitization-to-Float32 grades, validated by round-trip. For the low-precision devices the collision interval  $[-x^\dagger, x^\dagger]$  of Theorem 2 covers the whole axis, so they cannot fingerprint, but four to five significant figures is still ample for data liberation and for the coincidence-based forensics of Theorem 3. The honest boundary is that provenance is matplotlib-PDF territory, while data liberation spans the whole ecosystem.

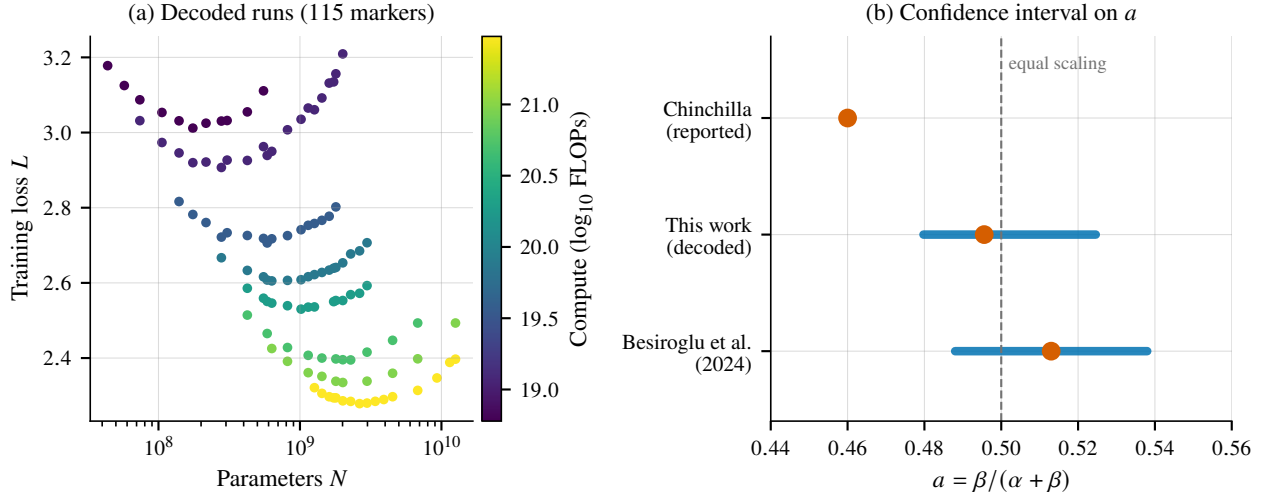


Figure 2: Confirming a published correction from the figure alone. (a) The training runs we recover from the vector figure of Hoffmann et al. [11]: 115 markers, each a model’s final training loss  $L$  against its parameter count  $N$ , coloured by training compute in FLOPs. At a fixed compute budget the runs form one isoFLOP profile, whose envelope fixes the compute-optimal model size; we plot our recovered data, not the published image. (b) The exponent  $a = \beta / (\alpha + \beta)$  that sets how optimal model size scales with compute, where  $a \approx 0.5$  means parameters and training data should grow together. Bars are confidence intervals and dots are point estimates. “Chinchilla (reported)” is the original parametric fit (their Approach 3); its interval (width  $\approx 0.001$ ) is a near-point, whereas our independent-refit bootstrap of the decoded data and the reanalysis of Besiroglu et al. [10] both give intervals more than forty times wider and mutually consistent around  $a \approx 0.5$ . Our role is to reproduce that published correction directly from the figure.

## 9 Application

A safe way to show what the method is for is to revisit a question that is already public, already in the literature, and entirely about a number rather than about conduct: how wide the confidence interval on the Chinchilla compute-optimal exponent should be. Besiroglu et al. [10] reanalysed the scaling-law fit of Hoffmann et al. [11] and argued that the reported interval on the exponent  $a = \beta / (\alpha + \beta)$  was implausibly tight, a point the original authors acknowledged. We take that published correction as our starting point and ask a narrow methodological question: can it be confirmed directly from the figure, at the renderer’s precision, without re-running anyone’s experiments?

It can. The per-run points behind the relevant isoFLOP figure were not released as a table, so the figure is their only public record. We decode 115 markers from the vector figure, calibrate from its logarithmic parameter axis and linear loss axis (Section C), and refit the reported model  $L = E + A/N^\alpha + B/D^\beta$  (Figure 2a). Recovering all 115 points is a single automatic pass over the figure; tracing that many overlapping markers by hand at comparable precision would be slow and would itself inject the digitization noise our reading is meant to exclude. Bootstrapping on the authors’ own protocol gives a confidence interval on  $a$  of width about 0.045, more than forty times the reported  $\approx 0.001$  and in close agreement with the reanalysis of Besiroglu et al. [10] (Figure 2b). Because we read the figure at its storage precision rather than by hand, our result removes digitization noise as a possible objection to that reanalysis: the wide interval is present in the authors’ own plotted points, not an artefact of imprecise tracing.

Two points keep this in proportion. First, the scaling law’s headline finding, that parameters and training data should scale together with  $a \approx 0.5$ , is untouched: our central estimate  $a \approx 0.50$  agrees with it, and only the stated precision of one exponent is at issue. Second, the narrow interval has an innocent and reproducible explanation, which we record as an observation and not a charge: it reappears when each bootstrap resample is warm-started from the single converged fit instead of refit independently, a common shortcut. We present the case in this form, as the independent confirmation of an existing, acknowledged correction, because that is the method’s intended use: liberating the data of record so that published conclusions can be checked, combined, and, where warranted, refined, with every recovered value offered as a candidate for review (Section 10).

## 10 Responsible use

Because this work recovers data that authors did not explicitly release, and because its forensic mode can surface apparent inconsistencies, we adopt explicit safeguards.

- **Candidates, not verdicts.** Every output, whether a recovered dataset, a cross-figure match, or a failed re-render certificate, is a candidate for human review, accompanied by its uncertainty (Section 4) and its coincidence bound (Section 5). The system makes no accusation, and we name no individual or paper as fraudulent. The one named figure we analyse in depth (Section 9) concerns a published, already-adjudicated numerical dispute, not conduct.
- **Read-only and reproducible.** All external access is read-only; we take no outward or irreversible action. The verifier is deterministic, so any reported result can be independently re-derived from the same input.
- **Provenance, not surveillance.** We decline privacy-sensitive uses. Where a capability could be misused, for instance de-anonymizing an author through render fingerprints, we evaluate it only on synthetic data and report it as a measured limit, not as a tool.
- **Corrections through normal channels.** A recovered correction (Section 9) is a scientific contribution to be raised through comment, contact with authors, or reanalysis, not a public allegation.

**Distribution and copyright.** We release the verifier and a metadata-only resource index. We do not redistribute any third-party figure or PDF; published figures remain the property of their authors and publishers, and our artifacts reference them by identifier rather than reproducing them. Self-generated figures used for ground-truth tests are released in full, since we own them.

## 11 Conclusion

Data-bearing vector figures are a high-bit container that the literature has been treating as a picture. We gave a precision theory that bounds how much of their contents can be recovered (bit-exact `Float32` for `matplotlib` markers, calibration-limited three-to-four significant figures end-to-end), and a no-collision theory under which recovery is injective away from a characterized, vanishing interval near zero and an apparent match is evidence rather than coincidence. An automatic verifier realizes both, recovering data with no human in the loop and certifying the result by re-rendering its markers, lines, and ticks to the original. With no ground truth in the loop the decoder reproduces external archives to  $\sim 10^{-9}$  (markers) and  $\sim 5 \times 10^{-4}$  (polylines), and on a single famous figure it independently reproduces a published correction to a scaling-law confidence interval. A map across renderers and export formats delimits where each guarantee holds.

Together these turn the three deficiencies of hand-digitization (low precision, low automation, no verification) into provable, automatic, certifiable properties, for the class of figures that carry their data in vector form. Our aim is to make figure-encoded data a first-class, checkable part of the scientific and technical record.

## Code and data availability

The verifier `FIGVERIFY`, together with its unit tests and self-contained fixtures, the renderer-precision measurements, and a metadata-only index of the figures analysed, is available under the MIT license at <https://github.com/Bowen-Sun-0728/figverify>. It installs as a command-line tool (`classify`, `extract`, `verify`) and reproduces the experiments reported here. No third-party figures or PDFs are redistributed (Section 10).

## References

- [1] Ankit Rohatgi. WebPlotDigitizer. <https://automeris.io/WebPlotDigitizer>, 2017.
- [2] John D. Hunter. Matplotlib: A 2d graphics environment. *Computing in Science & Engineering*, 9(3):90–95, 2007. doi: 10.1109/MCSE.2007.55.
- [3] Damien Masson, Sylvain Malacria, Daniel Vogel, Edward Lank, and Géry Casiez. Chartdetective: Easy and accurate interactive data extraction from complex vector charts. In *Proceedings of the 2023 CHI Conference on Human Factors in Computing Systems*, CHI '23, New York, NY, USA, 2023. Association for Computing Machinery. ISBN 9781450394215. doi: 10.1145/3544548.3581113. URL <https://doi.org/10.1145/3544548.3581113>.

- [4] echemdb. svgsdigitizer. <https://github.com/echemdb/svgsdigitizer>, 2022.
- [5] James J. Hamlin. Vector graphics extraction and analysis of electrical resistance data in nature volume 586, pages 373-377 (2020), 2022. URL <https://arxiv.org/abs/2210.10766>.
- [6] Elisabeth M. Bik, Arturo Casadevall, and Ferric C. Fang. The prevalence of inappropriate image duplication in biomedical research publications. *mBio*, 7(3):10.1128/mbio.00809-16, 2016. doi: 10.1128/mbio.00809-16. URL <https://journals.asm.org/doi/abs/10.1128/mbio.00809-16>.
- [7] IEEE. IEEE Standard for Floating-Point Arithmetic. *IEEE Std 754-2019 (Revision of IEEE 754-2008)*, pages 1–84, 2019. doi: 10.1109/IEEESTD.2019.8766229.
- [8] Planck Collaboration, N. Aghanim, et al. Planck 2018 results: Vi. cosmological parameters. *Astronomy & Astrophysics*, 641:A6, September 2020. ISSN 1432-0746. doi: 10.1051/0004-6361/201833910. URL <http://dx.doi.org/10.1051/0004-6361/201833910>.
- [9] NOAA Global Monitoring Laboratory. Trends in co2, ch4, n2o, sf6. <https://gml.noaa.gov/ccgg/trends/>, 2026.
- [10] Tamay Besiroglu, Ege Erdil, Matthew Barnett, and Josh You. Chinchilla scaling: A replication attempt, 2024. URL <https://arxiv.org/abs/2404.10102>.
- [11] Jordan Hoffmann, Sebastian Borgeaud, Arthur Mensch, Elena Buchatskaya, Trevor Cai, Eliza Rutherford, Diego de Las Casas, Lisa Anne Hendricks, Johannes Welbl, Aidan Clark, Tom Hennigan, Eric Noland, Katie Millican, George van den Driessche, Bogdan Damoc, Aurelia Guy, Simon Osindero, Karen Simonyan, Erich Elsen, Jack W. Rae, Oriol Vinyals, and Laurent Sifre. Training compute-optimal large language models, 2022. URL <https://arxiv.org/abs/2203.15556>.

## A Proof of the extraction-precision ceiling

We prove Theorem 1, in the setup fixed there: the stored coordinate is  $\tilde{u} = u + \eta$  with  $|\eta| \leq \frac{1}{2}\Delta_s$  on the grid Equation (2); the map recovered from the ticks is  $\hat{a} = a(1 + \delta_a)$  and  $\hat{b} = b + \Delta_b$  with  $|\delta_a| \leq \varepsilon$  and  $|\Delta_b| \leq \varepsilon|b|$ ; and recovery inverts it as  $\hat{v} = (\tilde{u} - \hat{b})/\hat{a}$ .

*Proof.* Substitute  $\tilde{u} = av + b + \eta$  and the calibration estimates:

$$\hat{v} = \frac{av + b + \eta - (b + \Delta_b)}{a(1 + \delta_a)} = \frac{av + \eta - \Delta_b}{a(1 + \delta_a)} = \left(v + \frac{\eta}{a} - \frac{\Delta_b}{a}\right)(1 + \delta_a)^{-1}.$$

Expanding  $(1 + \delta_a)^{-1} = 1 - \delta_a + O(\delta_a^2)$  and discarding products of two small quantities ( $\eta\delta_a$  and  $\Delta_b\delta_a$  are  $O(\varepsilon^2)$  because  $\eta$  is already at the storage scale),

$$\hat{v} - v = -v\delta_a + \frac{\eta}{a} - \frac{\Delta_b}{a} + O(\varepsilon^2).$$

Taking absolute values and using the triangle inequality with the bounds on  $\eta$ ,  $\delta_a$ , and  $\Delta_b$ ,

$$|\hat{v} - v| \leq \frac{|\eta|}{|a|} + |v||\delta_a| + \frac{|\Delta_b|}{|a|} \leq \frac{\Delta_s}{2|a|} + \varepsilon|v| + \varepsilon\left|\frac{b}{a}\right| + O(\varepsilon^2),$$

which is the claim.  $\square$

**Corollary 1** (Bit-exact recovery). *Suppose calibration is exact ( $\varepsilon = 0$ ) and the data are Float32 numbers. If the storage step is below half the floating-point ULP across the plotted range,  $\frac{1}{2}\Delta_s/|a| < \frac{1}{2}\text{ulp}(v)$  for all plotted  $v$ , then  $\hat{v} = v$  bit-for-bit after rounding to Float32.*

*Proof.* By Theorem 1 with  $\varepsilon = 0$ ,  $|\hat{v} - v| \leq \Delta_s/(2|a|) < \frac{1}{2}\text{ulp}(v)$ , so  $v$  is the unique Float32 number within half an ULP of  $\hat{v}$ ; rounding  $\hat{v}$  to Float32 returns  $v$ .  $\square$

For matplotlib’s PDF backend,  $\Delta_s = 10^{-10}$  in the transformed unit gives  $B_{\text{extract}} = \log_2(\text{span}/\Delta_s) \approx 42$  bits, comfortably above the 24-bit Float32 significand everywhere except the vanishing near-zero interval of Theorem 2, so the hypothesis of Corollary 1 holds away from that interval and marker recovery is bit-exact when calibration is tight (Section 7).

## B Proofs of the no-collision properties

### B.1 Injectivity and the collision interval

*Proof of Theorem 2.* Two data values  $v_1 \neq v_2$  are stored as  $\tilde{u}_i = \Delta_s \text{round}(u_i/\Delta_s)$  with  $u_i = av_i + b$ . If  $|u_1 - u_2| = |a||v_1 - v_2| > \Delta_s$ , then  $u_1$  and  $u_2$  cannot round to the same grid value, so  $\tilde{u}_1 \neq \tilde{u}_2$  and recovery distinguishes them; conversely if the device separation is at most  $\Delta_s$  they may share a grid value. Hence recovery is injective on data whose consecutive separations exceed  $\Delta_s/|a|$ .

Now let the data be Float32 numbers. The representable grid near magnitude  $|v|$  has spacing  $\text{ulp}(v) = 2^{\lfloor \log_2 |v| \rfloor - 23}$ . Neighbouring representable values are individually resolvable iff their device separation exceeds the storage quantum,

$$|a| \text{ulp}(v) > \Delta_s \iff 2^{\lfloor \log_2 |v| \rfloor - 23} > \frac{\Delta_s}{|a|} =: \delta.$$

Writing  $\lfloor \log_2 |v| \rfloor > 23 + \log_2 \delta$  and using  $|v| \geq 2^{\lfloor \log_2 |v| \rfloor}$  gives the threshold

$$|v| > x^\dagger, \quad x^\dagger = 2^{\lfloor \log_2(2\delta) \rfloor + 24} \approx \delta 2^{24} = \frac{\Delta_s}{|a|} 2^{24},$$

where the factor 2 inside the floor accounts for round-to-nearest. Thus the non-resolvable set is the dyadic interval  $[-x^\dagger, x^\dagger]$ , establishing Equation (4).  $\square$

**Numerical size.** With  $\delta = \Delta_s/|a|$  expressed as a fraction of the axis range,  $x^\dagger \approx \delta 2^{24}$ . For matplotlib PDF,  $\delta$  is small enough that  $x^\dagger \approx 4 \times 10^{-6}$  of the range; for R’s PDF devices  $\delta$  is large enough that  $x^\dagger$  exceeds the range, so no datum is resolvable at the Float32 level, consistent with Table 1.

### B.2 The coincidence bound

*Proof of Theorem 3.* Model each effective coordinate, after the entropy gate of Section 5 has removed degenerate, low-cardinality, or structured values, as a draw from a distribution that is, to an adversary trying to produce a chance match, no more concentrated than uniform over its  $2^b$  resolvable cells. For two independent draws, the probability of landing in the same cell (within the matching tolerance of one cell) is at most  $2^{-b}$ . A point has two coordinates, assumed independent, so a single point matches with probability at most  $2^{-2b}$ . The  $n$  points are independent, so

$$\Pr[\text{all } n \text{ points match}] \leq (2^{-2b})^n = 2^{-2nb}.$$

$\square$

**Remarks.** (i) The bound rests on the entropy gate, which fixes  $b$  as a coordinate’s honest effective entropy by excluding degenerate, low-cardinality, and structured sequences. What remains places at most  $2^{-b}$  of its mass on any one resolvable cell (min-entropy at least  $b$ ), and that is what caps the chance-collision probability at  $2^{-b}$ . Concentration the gate fails to remove would raise the chance of an accidental match, not lower it, so the gate is deliberately conservative; genuinely shared data match regardless. (ii) The exponent scales linearly in both the number of points  $n$  and the per-coordinate bits  $b$ , so even modest figures give overwhelming evidence:  $n = 20, b = 10$  yields  $2^{-400}$ . (iii) For a re-render certificate (Section 6) the “match” is over every data-bearing primitive simultaneously, every marker, vertex, and tick, so  $n$  is the full point count and the bound is far below any machine epsilon, which is why agreement on those primitives is treated as proof of faithful recovery. (iv) The exponent counts two independent coordinates per point,  $2b$  bits; for a functional relation  $y = f(x)$  a point carries closer to  $b$ , so the honest exponent is  $nb$ , still far below machine epsilon for any non-trivial figure.

## C Recovering the affine map from ticks

The calibration step of Theorem 1 recovers the affine map  $(a, b)$  of Equation (1) using only the axis ticks the renderer itself drew, with no axis limits, data range, or metadata assumed. Because this step, not the storage quantum, sets the precision actually achieved (Section 4), we give it in full. It has four stages.

**Panels.** A single content stream may hold several subplots, so we first segment the page into panels. We take the rectangles the renderer drew for the axis frames, keep those whose area is a sizable but not page-filling fraction of the page, and de-overlap them greedily, rejecting a candidate that overlaps an accepted panel by more than a set fraction. Each marker is later assigned to the panel whose frame contains it, and every panel is calibrated on its own.

**Tick labels.** For each panel we collect the text spans the renderer placed just below the bottom edge as candidate  $x$  labels and just left of the frame as candidate  $y$  labels, each tagged with the device coordinate of its bounding box. Turning a label into a value is where a naive parser fails, and three cases recur in scientific figures. A logarithmic label is drawn as a base “10” with a raised, smaller exponent; we recombine the pair into  $10^k$ , but only when the exponent span is set smaller and lifted above the baseline, so that two ordinary neighbouring ticks such as “10” and “15” are never fused into a spurious  $10^{15}$ . Engineering labels such as “100M”, “1B”, or “10T” are expanded through their SI suffixes, and scientific text such as “6e18” is read directly. We normalise the Unicode minus sign, the multiplication sign, and thousands separators before parsing.

**Linear or logarithmic fit.** From the cleaned (position, value) pairs of one axis we fit two models by least squares, a linear map  $v = p + qu$  and a logarithmic map  $\log_{10} v = p + qu$  (the scale and offset  $(a, b)$  of Equation (1) follow by inversion), and keep whichever has the smaller residual, measured in device points. The residual doubles as a quality gate: a panel whose best fit exceeds a few points, or that yields fewer than two parseable ticks on an axis, is reported as uncalibrated rather than guessed. The chosen map is inverted to decode each marker (Section 6); a logarithmic axis decodes as  $10^{p+qu}$ .

**Where the calibration error comes from.** With the fit in hand, the relative error  $\varepsilon$  of Equation (3) is set not by geometry but by the tick labels. A printed label is a rounded display of the true tick value: an axis annotated “0.5” fixes that tick only to the precision the author chose to print, and the affine map inherits that uncertainty. The device positions of the ticks are themselves stored coordinates, quantised at  $\Delta_s$ , which is negligible beside label rounding, while the fit residual across several ticks is the third and usually smallest contribution. This is why Section 4 finds calibration, not storage, to be the bottleneck, and why anything that adds independent constraints, more ticks, a declared axis transform, or author-supplied limits, drives the achievable precision back toward the storage floor. When the plotted data are `Float32` and the axis carries enough ticks,  $\varepsilon$  falls below the floating-point ULP and recovery is bit-exact (Corollary 1).